Fluid Model of Central Cell Plasma in a Tandem Mirror

L.L. Lao and R.W. Conn

March 1979

UWFDM-294

FUSION TECHNOLOGY INSTITUTE

UNIVERSITY OF WISCONSIN

MADISON WISCONSIN

Fluid Model of Central Cell Plasma in a Tandem Mirror

L.L. Lao and R.W. Conn

Fusion Technology Institute
University of Wisconsin
1500 Engineering Drive
Madison, WI 53706

http://fti.neep.wisc.edu

March 1979

UWFDM-294

Fluid Model of Central Cell Plasma in a Tandem Mirror

L. L. Lao

R. W. Conn

March 1979

UWFDM-294

Nuclear Engineering Department
University of Wisconsin
Madison, Wisconsin 53706

Abstract

A fluid model to describe plasma confined in the central cell of a tandem mirror machine is developed. The model properly includes axial losses, radial losses and the interaction of electrons with all ionic species either in the central cell or in the plugs. The density and ion energy of the plug plasma are self-consistently calculated using either fixed or calculated spatial profiles. Illustrative calculations are performed for a specific confinement experiment, the Wisconsin tandem mirror device, PHAEDRUS, by using classical radial transport coefficients. The results show that the radial profile of various central-cell plasma parameters can be controlled by tailoring the plug plasma density profile. If the radial transport coefficients are eight to ten times the classical values, the losses will be mainly in the radial direction. For PHAEDRUS, the results are not sensitive to the boundary conditions used at the plasma edge.

I. Introduction

A particle has an axial confinement time of the order of an ion-ion collision time, τ_{ii}, in a conventional mirror confined plasma and on this time scale, radial diffusion is too slow a process to play any role. The maximum Q value in such a mirror is limited to about 1. In a tandem mirror,[1,2] the axial confinement time of the central-cell plasma is greater than τ_{ii} by the factor $\frac{ze\phi_c}{T_c} \exp \frac{ze\phi_c}{T_c}$. The overall confinement time can be increased sufficiently to permit Q values well in excess of 1 but this raises the prospect that radial transport may compete with axial losses. We list in Table 1 the major plasma parameters of several tandem mirror devices. These include TMX,[3] a neutral beam heated tandem mirror experiment operating at the Lawrence Livermore Laboratory, PHAEDRUS,[4] an RF heated tandem mirror experiment operating at the University of Wisconsin, and two conceptual tandem mirror reactor designs.[5,6] The calculated axial confinement times for these devices are compared in Table 2 with estimates for the radial confinement time based on either classical or Bohm-like transport. One can see that for present day experimental tandem devices, the classical radial confinement time is about an order of magnitude larger than the axial confinement time. On the other hand, Bohm-like radial transport would be substantially faster than the axial loss rate. In reactors, the axial alpha particle confinement time is an order of magnitude larger than the classical radial confinement time because the alphas are multiply charged and well confined electrostatically. Furthermore, recent calculations for the guiding-center orbits of particles in a quadrupole-field stabilized tandem mirror show that the rapid twisting and bunching of the magnetic field lines

Table 1

	TMX[4]	PHAEDRUS[5]	TMR-LLL[6]	TMR-UW[7]
$n_p(cm^{-3})$	$5x10^{13}$	$8x10^{12}$	$8.6x10^{14}$	$4x10^{14}$
$n_c(cm^{-3})$	$1.2x10^{13}$	$3x10^{12}$	$1.1x10^{14}$	$4x10^{13}$
E_p(keV)	26	2	880	955
T_e(keV)	.20	.050	42	44
T_c(keV)	0.080	.015	30	40
ϕ_e(keV)	1.1	.26	260	265
ϕ_c(keV)	.29	.05	90	103
R_c(cm)	31	17	120	240
L_c(cm)	550	400	10000	18400
$R_p(0)$ (cm)	7	7	50	69
L_p(cm)	40	100	100	138
Q	-	-	5	10
$(n\tau)_p$ cm^{-3}-s	$3x10^{11}$	$1.5x10^{10}$	$2.5x10^{14}$	$3.6x10^{14}$

Table 2

Various Characteristic Times for Central-Cell Ions

($n\tau$ in units of cm^{-3}-s)

	TMX[4]	PHAEDRUS[5]	TMR-LLL[6]	TMR-UW
$(n\tau)_c^p$	3×10^{11}	2.5×10^{10}	8×10^{14}	8×10^{14}
$(n\tau)_c^K$	1×10^{11}	9×10^{9}	3×10^{14}	3.4×10^{14}
$(n\tau)_\perp^p$	4×10^{12}	7×10^{11}	6×10^{17}	3×10^{17}
$(n\tau)_\perp^K$	2×10^{11}	2×10^{10}	1.6×10^{16}	1.3×10^{16}
$(n\tau)_{Bohm}$	4×10^{9}	3.6×10^{9}	6×10^{10}	2.1×10^{10}
$(n\tau)_\parallel^\alpha$	-	-	3.8×10^{16}	2.5×10^{16}
$(n\tau)_\perp^\alpha$	-	-	2.5×10^{15}	5×10^{15}
$(n\tau)_{\alpha_\perp}^{.1}$	-	-	7×10^{14}	6×10^{14}
$(n\tau)_{th}^\alpha$	-	-	1.5×10^{14}	1.6×10^{14}

$(n\tau)_c^p$ = axial ion particle confinement time; $(n\tau)_c^K$ = axial ion energy confinement time; $(n\tau)_\perp^p$ = classical radial ion confinement time; $(n\tau)_\perp^K$ = classical radial ion conduction time; $(n\tau)_{Bohm}$ = Bohm diffusion time; $(n\tau)_\parallel^\alpha$ = axial alpha particle confinement time; $(n\tau)_\perp^\alpha$ = classical alpha particle radial confinement time; $(n\tau)_{\alpha_\perp}^{.1}$ = radial alpha diffusion time required to maintain $\frac{n_\infty^\alpha}{n_i} = .1$; $(n\tau)_{th}^\alpha$ = alpha particle thermalization time.

in the transition region between the minimum-B end plugs and the uniform central solenoid causes particles to drift radially.[7] If the plugs are joined with their elliptical flux tubes facing each other, the radial drift, $\frac{\delta r}{r}$, is of the order 1. If the plugs are joined with their flux tubes oriented at 90° to one another and if the azimuthal drift, $\Delta\Psi$, of a particle in one bounce through the central cell is small ($\Delta\Psi \ll 1$), the radial drifts in the two transition regions cancel each other to the first order. If the central-cell plasma beta, β_c, is high (~O(1)) and if the ambipolar potential, ϕ_e, of the central cell with respect to ground has a strong radial dependence, local cancellation of the azimuthal drifts caused by the gradient in the magnetic field and the radial electric field can take place. This leads to neoclassical diffusion.[8] If β_c is low but ϕ_e has a strong radial dependence, an ion can drift azimuthally 90° or more in one bounce through the central cell and can diffuse resonantly in the radial direction.[9] However, unlike the classical case, these two types of diffusion are caused by like particle collisions rather than unlike particle collisions. Such diffusion can be large and may not be negligible compared to axial losses.

All these issues relate to radial transport in the central cell plasma and have been the motivation for us to develop a physical model for a tandem-mirror plasma which properly includes the radial and axial losses as well as the interaction of the electron fluid with various ionic species in either the central cell or in the plugs.

In the next section, we give a description of the plasma model and a derivation of the basic equations. We then briefly consider the transport coefficients which close these equations and finally as an example, we discuss numerical solutions to this set of non-linear coupled differential equations using plasma parameters characteristic of the Wisconsin tandem device PHAEDRUS.

II. Plasma Model

Each plasma species, a, in a tandem mirror can be described using the distribution function $f_a(\bar{r},\bar{V},\bar{t})$ which satisfies the Boltzman equation:

$$\frac{\partial f_a}{\partial t}(\bar{r},\bar{V},t) + \bar{V}\cdot\frac{\partial f_a}{\partial \bar{r}} + q_a\left(\bar{E} + \frac{\bar{V}\times\bar{B}}{C}\right)\cdot\frac{\partial}{\partial \bar{V}} f_a$$

$$= \sum_b C_{ab}(f_a,f_b) \tag{2.1}$$

where C_{ab} is the Coulomb collision operator given by

$$C_{ab} = -\frac{2\pi q_a^2 q_b^2}{m_a}\ell n\Lambda_{ab}\frac{\partial}{\partial V_\alpha}\int d^3V'\left[\frac{f_a(\bar{V})}{m_b}\frac{\partial f_b(\bar{V}')}{\partial V'_\beta}\right.$$

$$\left. - \frac{f_b(\bar{V}')}{m_a}\frac{\partial}{\partial V_\beta} f_a(\bar{V})\right] W_{\alpha\beta}(\bar{V}-\bar{V}') \tag{2.2}$$

$$W_{\alpha\beta}(\bar{y}) = \frac{1}{y^3}(y^2\delta_{\alpha\beta} - y_\alpha y_\beta) \tag{2.3}$$

II-A. Central-Cell Ions

The bulk of the central-cell ions in a tandem mirror are confined electrostatically so that their distribution function is close to a Maxwellian. They can thus be considered as a fluid having a local temperature $T_a(\bar{r},t)$ and a density $n_a(\bar{r},t)$ which satisfy the moment equations:

$$\frac{\partial}{\partial t} n_a(\bar{r},t) + \bar{\nabla} \cdot \bar{\Gamma}_a = S_a \tag{2.4}$$

$$\frac{\partial}{\partial t}\left(\frac{3}{2} n_a T_a\right) + \bar{\nabla} \cdot \left(\frac{3}{2} T_a \bar{\Gamma}_a + \bar{Q}_a\right) + n_a T_a \bar{\nabla} \cdot \bar{U}_a + \pi^a_{\alpha\beta} \frac{\partial U_{a\alpha}}{\partial x_\beta} = \sum_{b\neq a} P_{ab} + P^a_{aux} \tag{2.5}$$

where

$$n_a(\bar{r},t) = \int d^3V\, f_a(\bar{r},\bar{V},t) \tag{2.6}$$

$$\bar{U}_a(\bar{r},t) = \frac{1}{n_a} \int d^3V\, \bar{V} f_a(\bar{r},\bar{V},t) \tag{2.7}$$

$$\bar{\Gamma}_a = n_a \bar{U}_a \tag{2.8}$$

$$T_a = \frac{1}{n_a} \int d^3V\, \frac{1}{2} m_a (\bar{V} - \bar{U}_a)^2 f_a(\bar{r},\bar{V},t) \tag{2.9}$$

$$\bar{Q}_a = \int d^3V\, \frac{1}{2} m_a (\bar{V} - \bar{U}_a)^2 (\bar{V} - \bar{U}_a) f_a(\bar{r},\bar{V},t) \tag{2.10}$$

S_a is the particle source for species a, P^a_{aux} is the auxiliary heating term for species a, and P_{ab} is the rethermalization term between plasma species a and b.

Since the magnetic field is solenoidal over most of the central-cell volume, it can be approximated by a square well. There is then no azimuthal dependence in configuration space and the axial dependence is eliminated by integrating equations (2.4) and (2.5) over a differential flux tube which has radius r in the central cell and R in the plug (Fig. 1). Neglecting the compressive flow term, $n_a T_a \bar{\nabla} \cdot \bar{U}_a$, and the viscosity term, $\pi^a_{\alpha\beta} \frac{\partial U_{a\alpha}}{\partial x_\beta}$, we have

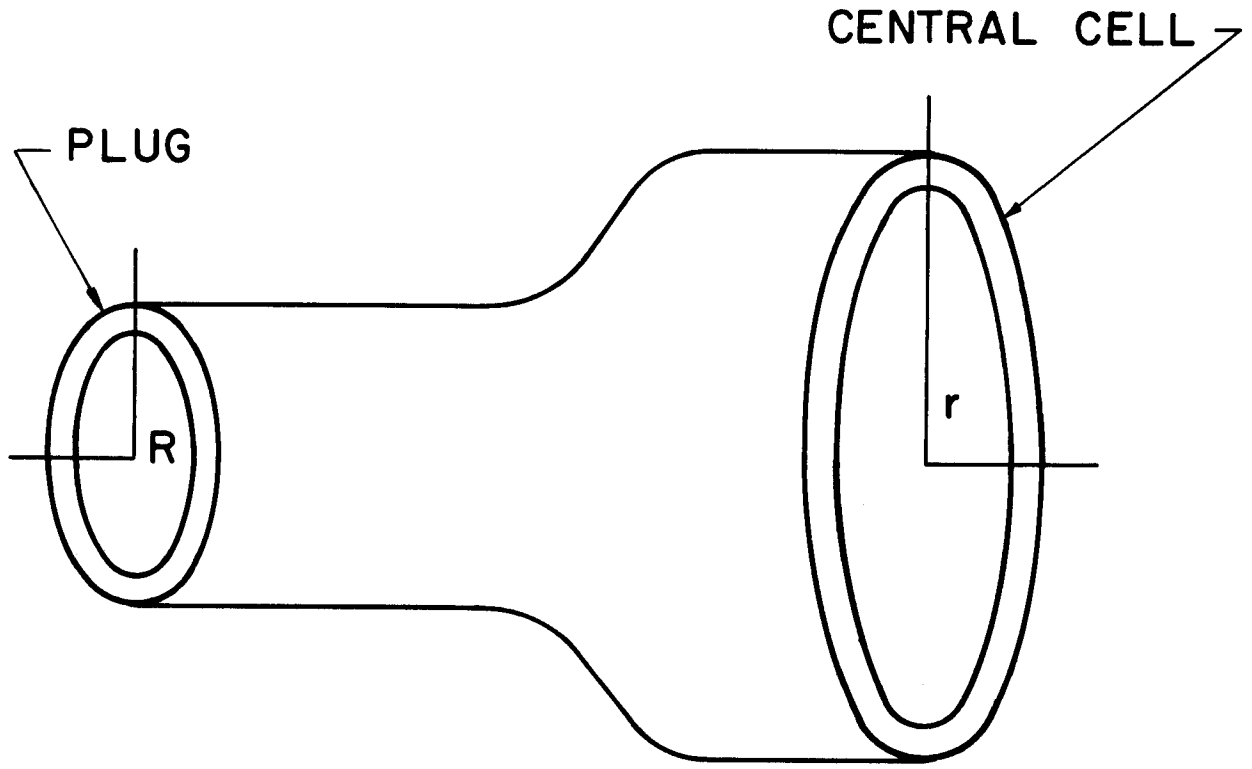

Fig. 1. Mapping of the central cell into the plug

$$\frac{\partial}{\partial t} n_a(r,t) = - \frac{1}{r} \frac{\partial}{\partial r} (r\Gamma_a) - \frac{n_a^2}{2} \langle\sigma V\rangle_{DT} \gamma_{DT} - L_{\perp}^{a} + S_a \tag{2.11}$$

$$\frac{\partial}{\partial t}(\frac{3}{2} n_a T_a) = \frac{1}{4} n_a^2 \langle\sigma V\rangle_{DT} E_\alpha U_\alpha^a \gamma_{DT} - \frac{1}{r} \frac{\partial}{\partial r} r(Q_a + \frac{3}{2} T_a \Gamma_a)$$

$$+ \sum_{b \neq a} P_{ab} + P_{aux}^{a} - Q_{\perp}^{a} - Q_{cx}^{a} \tag{2.12}$$

where γ_{DT} is 1 for DT plasma and 0 otherwise, E_α is the initial fusion alpha particle energy (3.5 MeV,) and U_α^a is the fraction of alpha particle energy which is transferred to species a as the alpha slows down. Q_{cx}^{a} is the charge exchange loss term for species a, and $L_{\perp}^{a}$ and $Q_{\perp}^{a}$ are the axial particle and energy losses. Analytic expressions for $L_{\perp}^{a}$ and $Q_{\perp}^{a}$ have been obtained by several authors.[10-12] For a multi-species plasma in a square well, one can write,[11]

$$L_{\perp}^{a} = \frac{n_a}{\tau_{\perp}^{a}} \tag{2.13}$$

$$Q_{\perp}^{a} = \frac{z_a e\phi_c + T_a}{\tau_{\perp}^{a}} \tag{2.14}$$

where

$$\tau_{\perp}^{a} = T_a \frac{\sqrt{\pi}}{4} G(H_a R_c) \frac{1}{H_a I(\frac{T_a}{z_a e\phi_c})} \frac{z_a e\phi_c}{T_a} \exp(\frac{z_a e\phi_c}{T_a}) \tag{2.15}$$

$$\tau_a = \frac{m_a^{1/2} T_a^{3/2}}{\sqrt{2}\,\pi z_a^2 e^4} \frac{1}{\sum_b n_b z_b^2 \ell n\Lambda_{ab}} \tag{2.16}$$

$$H_a = \frac{\sum_b n_b z_b^2 \ell n\Lambda_{ab}}{\sum_b n_b z_b^2 \frac{m_a}{m_b} \ell n\Lambda_{ab}} \tag{2.17}$$

$$I(x) = \begin{cases} 1 + \frac{(\pi x)^{1/2}}{2} \exp(\frac{1}{x})[1 - \mathrm{erf}(x^{-1/2})] & x < 1 \\ \frac{1 + \frac{x}{2}}{1 + \frac{x^2}{4}} & x > 1 \end{cases} \tag{2.18}$$

$$G(x) = \frac{2x + 1}{2x} \ln(4x + 2) \tag{2.19}$$

and

$$e\phi_c = T_e \ln(\frac{n_{ep}}{n_{ec}}) . \tag{2.20}$$

R_c is the mirror ratio between the plug mid-plane and the central-cell mid-plane and n_{ep} and n_{ec} are the plug and central cell electron densities, respectively.

II-B. Electrons

Electrons in a tandem mirror are confined electrostatically. Therefore, their distribution function is close to a Maxwellian and they can be considered as a fluid having a local temperature $T_e(\bar{r},t)$ and local density $n_e(\bar{r},t)$. Because of their frequent collisions, electrons move rapidly among the three cells and can be characterized by a uniform temperature T_e along each field line from the central cell to the plug. The electrons take energy from the plug ions and give energy to central cell ions. As before, the magnetic field in the central cell and the plugs is approximated by three square wells. The electron energy balance equation (2.5) is then integrated over a differential flux tube which has a radius r in the central-cell and R in the plug (Fig. 1) to obtain:

$$\frac{\partial}{\partial t}\left(\frac{3}{2} n_{ec} T_e + 3V_{pc} n_{ep} T_e\right) = \frac{1}{4} n_c^2 \langle \sigma V \rangle_{DT} E_\alpha U_\alpha^e \gamma_{DT}$$

$$- \frac{1}{r} \frac{\partial}{\partial r} r\left(Q_e + \frac{3}{2} T_e \Gamma_e\right) + \sum_{b \neq e} P_{eb} + P_{aux}^e$$

$$- Q_{\parallel}^e - Q_{rad} \tag{2.21}$$

where

$$n_{ec} = n_c + 2n_\alpha + zn_z, \tag{2.22}$$

$$n_{ep} = n_p, \tag{2.23}$$

n_c, n_α, and n_z are the central cell ion, alpha, and impurity density, respectively, n_p is the plug ion density, and V_{pc} is defined as $V_{pc} = \frac{\text{differential flux tube volume in each plug}}{\text{differential flux tube volume in the central cell.}}$ Q_{rad} represents bremsstrahlung, line, recombination, and synchrotron radiation losses, and $Q_{\parallel}^e$ is the total axial electron energy loss rate from a differential flux tube in the plugs and in the central cell. This latter quantity can be written as[11]:

$$Q_{\parallel}^e = \frac{n_{ep}(\phi_e + \phi_c + T_e)\langle \zeta \rangle}{\tau_{eff}} \tag{2.24}$$

where

$$\langle \zeta \rangle = V_{pc}\left(1 + \frac{L_c}{2L_p} \frac{\ell n \Lambda_{eec}}{\ell n \Lambda_{eep}} \frac{n_{ec}}{n_{ep}} \frac{\phi_c + \phi_e}{\phi_e}\right) , \tag{2.25}$$

$$\tau_{eff} = \langle \tau \rangle \left(\frac{\left(1 + \langle \tau \rangle \frac{d}{dt}\left[(n_{ec} + V_{pc} n_{ep})\langle \phi \rangle\right] V_{pc}\right)}{n_{ep}(\phi_e + \phi_i + T_e)\langle \zeta \rangle} \right)^{-1} , \tag{2.26}$$

$$\langle \tau \rangle = \tau_{ep} \frac{\sqrt{\pi}}{4} \frac{\ell n(4\langle Z \rangle R_p + 2)}{\langle Z \rangle} \frac{e(\phi_e + \phi_c)}{T_e} \frac{(2\langle Z \rangle R_p + 1)}{2\langle Z \rangle R_p}$$

$$\times \frac{\exp\left(\frac{e(\phi_e + \phi_c)}{T_e}\right)}{I\left(\frac{e(\phi_e + \phi_c)}{T_e}\right)} , \tag{2.27a}$$

$$\langle \phi \rangle = \frac{\phi_c}{1 + V_{pc} \frac{n_{ep}}{n_{ec}}} , \tag{2.27b}$$

$$\tau_{ep} = \frac{m_e^{1/2} T_e^{3/2}}{\sqrt{2}\,\pi e^4 n_{ep} \ell n\Lambda_{eep}} \quad , \tag{2.28}$$

$$\langle Z \rangle = \frac{\zeta_p + \frac{n_{ec}}{n_{ep} V_{pc}} \frac{\phi_c + \phi_e}{\phi_e} \frac{\ell n\Lambda_{eec}}{\ell n\Lambda_{eep}} \zeta_c}{1 + \frac{n_{ec}}{n_{ep}} \frac{\phi_e + \phi_c}{\phi_e} \frac{L_c}{2L_p} \frac{\ell n\Lambda_{eec}}{\ell n\Lambda_{eep}}} \quad , \tag{2.29}$$

$$\zeta_c = \frac{1}{2}\left[1 + \frac{1}{n_{ec}} \sum_{\substack{\text{central} \\ \text{cell} \\ \text{ions}}} n_j z_j^2 \frac{\ell n\Lambda_{ej}}{\ell n\Lambda_{eec}}\right] \quad , \tag{2.30}$$

and

$$\zeta_p = \frac{1}{2}\left[1 + \frac{1}{n_{ep}} \sum_{\substack{\text{plug} \\ \text{ions}}} n_j z_j^2 \frac{\ell n\Lambda_{ej}}{\ell n\Lambda_{eep}}\right] \quad . \tag{2.31}$$

If the central cell volume, V_c, is sufficiently large relative to that of the plug, V_p, we can neglect electron scattering in the plugs and $Q_{\perp}^{e}$ is given by the simpler formula[11]:

$$Q_{\perp}^{e} = \frac{T_e + e\phi_e}{\tau_{\perp}^{e}} \tag{2.32}$$

where

$$\tau_{\perp}^{e} = \tau_{ec} \frac{\sqrt{\pi}}{4} G(H_e R_c) \frac{1}{H_e I(\frac{T_e}{e\phi_e})} \frac{e\phi_e}{T_e} \exp(\frac{e\phi_e}{T_e}) \quad , \tag{2.33}$$

$$\tau_{ec} = \frac{m_e^{1/2} T_e^{3/2}}{\sqrt{2}\,\pi e^4 n_{ec} \ell n\Lambda_{eec}} \quad , \tag{2.34}$$

and

$$H_e = \frac{1}{2}\left(1 + \sum_{\substack{\text{central} \\ \text{cell} \\ \text{ions}}} \frac{z_i^2 n_i \ell n\Lambda_{ei}}{n_{ec} \ell n\Lambda_{ee}}\right) \quad . \tag{2.35}$$

II-C. Plug Ions

The electron energy balance equation is coupled to the plug ion density, n_p, and ion energy, E_p, through the plug-ion and electron energy exchange terms and through the axial loss term. To describe the plug ions, we use a point model with fixed or varying radial profile shapes. These are described as following:

II-C-1. Fixed Radial Profile

The plug ions are assumed to have fixed density and energy radial profiles of the form

$$n_p(R) = (m+1)\bar{n}_p\left(1 - \left(\frac{R}{R_{max}}\right)^2\right)^m \tag{2.36}$$

$$E_p(R) = \left(\frac{m+n+1}{m+1}\right)\bar{E}_p\left(1 - \left(\frac{R}{R_{max}}\right)^2\right)^n \tag{2.37}$$

The average plug ion density $\bar{n}_p$ and plug energy $\bar{E}_p$ are given by the zero-dimensional particle and energy balance equations:

$$\frac{d\bar{n}_p}{dt} = -\frac{\bar{n}_p}{\tau_{\parallel}^p} + S_p \tag{2.38}$$

$$\frac{d}{dt}(\bar{n}_p\bar{E}_p) = -\frac{\bar{n}_p(\bar{E}_p - \frac{3}{2}\bar{T}_e)}{\tau_{drag}^p} - \frac{\bar{n}_p E_{out}}{\tau_{\parallel}^p}$$

$$+ \left(1 + \frac{\sigma_{cx}}{\sigma_i}\right)S_p E_{inj} - \frac{\sigma_{cx}}{\sigma_i} S_p\bar{E}_p + P_{aux}^p \tag{2.39}$$

where S_p is the plug ion source, E_{inj} is the plug source injection energy and E_{out} is the average energy carried out by each plug ion. E_{out} can be written as

$$E_{out} = h\frac{\bar{T}_e^{3/2}}{\bar{E}_p^{1/2}}$$

where h is a parameter that is usually obtained from Fokker-Planck calculations. σ_{cx} and σ_i in eqn. (2.39) are the charge exchange and total impact ionization cross sections, respectively, P_{aux}^{p} is the auxiliary plug ion heating term, and

$$\tau_{i}^{p} = \left(\frac{1}{\tau_{ii}^{p}} + \frac{1}{\tau_{ei}^{p}}\right)^{-1} \tag{2.40}$$

$$\tau_{ei}^{p} = C_1 \tau_{drag}^{p} \ell n\left(\frac{E_p}{\phi_e + \phi_c}\right) \tag{2.41}$$

$$\tau_{ii}^{p} = C_2 \frac{A_p^{1/2} \bar{E}_p^{3/2}}{z_p^2 \bar{n}_p \ell n \Lambda_{ii}} \log_{10} R_p \tag{2.42}$$

and

$$\tau_{drag}^{p} = C_3 \frac{T_e^{3/2}}{\bar{n}_p} \frac{1}{\ell n \Lambda_{ei}} \tag{2.43}$$

R_p is the plug mirror ratio; C_1, C_2 and C_3 are constants. For tandem mirror experiments where a plasma stream is required to stabilize the plug plasma, we use Cohen's DCLC model[13]: if the sum of the central cell and plug axial losses and any external stream source is insufficient to supply the stabilizing current, the plug axial loss is increased to make up the difference. The radius R of the flux tube in the plug is related to that in the central cell r (Fig. 1) by conservation of the magnetic flux:

$$\int_0^r B_c(x) x \, dx = \int_0^R B_p(y) y \, dy \tag{2.44}$$

where

$$B_c(r) = B_{co}\sqrt{1 - \beta_c(r)} \quad , \tag{2.45}$$

$$B_p(r) = \begin{cases} B_{po}\sqrt{1 - \beta_p(R)} & \text{long thin plug} \\ B_{po}\left(1 - \frac{\beta_p(R)}{2}\right) & \text{short flat plug} \end{cases} \tag{2.46}$$

The central cell plasma beta is

$$\beta_c(r) = \sum_{\substack{\text{central} \\ \text{cell}}} n_j(r)T_j(r)/\frac{B_{co}^2}{2\mu_o} \tag{2.47}$$

and the plug plasma beta is

$$\beta_p(R) = \frac{n_p(R)(.9\, E_p(R) + T_e(R))}{\frac{B_{po}^2}{2\mu_o}} \tag{2.48}$$

and B_{co} and B_{po} are the central cell and plug vacuum magnetic field strengths, respectively.

II-C-2. Varying Radial Profile Shape

In this model, the radial profile shape of n_p and E_p at each radius R is calculated using particle and energy balance equations similar to equations (2.38) and (2.39). The radius R is again related to r by conservation of magnetic flux using eqn. (2.44).

II-D. Ambipolar Potential $\phi_e(r)$

The ambipolar potential, $\phi_e(r)$, of the central cell with respect to ground is determined at each radius r by equating the total electron and ion fluxes from each differential flux tube:

$$\frac{n_{ep}^2(r)}{n_{ep}^{<\tau>}}<\zeta> + \frac{1}{r}\frac{\partial}{\partial r} r\, \Gamma_e = \frac{n_{ic}^2(r)}{(n\tau_{,,})_c^i} + \frac{2V_{pc}n_{ip}^2(r)}{(n\tau_{,,})_p^i}$$

$$+ \frac{1}{r}\frac{\partial}{\partial r} r\Gamma_i + \left(\frac{n_{\alpha c}^2(r)}{(n\tau_{,,})_c^\alpha} + \frac{1}{r}\frac{\partial}{\partial r} r\, \Gamma_\alpha\right)\gamma_{DT} \tag{2.49}$$

where n_{ic}, n_{ip}, $n_{\alpha c}$ are the central-cell ion, plug ion, and alpha densities, respectively.

II-E. Discussion

If the transport coefficients are known, equations (2.11 - 2.12), (2.21), (2.38), (2.39), and (2.49) form a closed set of equations. Given a set of initial conditions, they describe the time evolution of a tandem-mirror plasma with radial losses in the central cell and axial losses in both the plugs and the central cell. This model differs from that given by Ryutov and Stupakov[8] in the following ways: First, it properly includes both the axial and the radial losses of the central-cell plasma. Secondly, models of the end plug plasma are included. The plug plasma density and ion energy are calculated self-consistently from the particle and energy balance equations. Thus, it provides a proper description of the transfer of energy from the plug ions to the electrons and then from the electrons to the central-cell ions. Thirdly, instead of assuming the electron temperature, T_e, is uniform across the field lines, $T_e(r)$ is calculated from the electron energy balance equation. Finally, $\phi_e(r)$ is determined self-consistently by equating the total electron and ion fluxes from each differential flux tube. The modelling of the axial losses in the central cell of a tandem mirror is similar to the modelling of the parallel losses to a divertor in a tokamak.[19] The situation is more complicated in the tandem mirror however because of the presence of the two end plugs.

III. Transport Coefficients

The particle and heat fluxes can generally be written in terms of the temperature, density, and ambipolar potential gradients as

$$\bar{\Gamma}_j = -\left(D_{jn}\frac{\partial n}{\partial r} + D_{je}\frac{\partial T_e}{\partial r} + D_{ji}\frac{\partial T_c}{\partial r} + \mu_j\frac{\partial \phi_e}{\partial r}\right)\bar{e}_r \ , \tag{2.50}$$

$$\bar{Q}_j = -\left(\chi_{jn}\frac{\partial n}{\partial r} + \chi_{je}\frac{\partial T_e}{\partial r} + \chi_{ji}\frac{\partial T_c}{\partial r} + \eta_j\frac{\partial \phi_e}{\partial r}\right)\bar{e}_r \ . \tag{2.51}$$

The full set of transport coefficients for the central-cell plasma in a tandem mirror are not fully known except for classical scaling.

III-A. Classical Diffusion

Classically, the particle and the energy fluxes are driven by collisional momentum exchange, i.e., the friction force and the collisional change in the energy flux. They can be written as:[14-17]

$$\left|\begin{array}{c}\bar{Q}_e\\ \bar{Q}_i\\ \bar{\Gamma}_i\\ \bar{\Gamma}_\alpha\end{array}\right|_r = \bar{\bar{F}} \left|\begin{array}{c}\nabla T_e\\ \nabla T_c\\ \nabla n_c\\ \nabla n_\alpha\end{array}\right|_r \tag{3.1}$$

where the matrix elements of $\bar{\bar{F}}$ are given by:

$$F_{11} = -7.57 \times 10^{-5}\ \frac{n_e^2\ \ell n\Lambda}{T_e^{1/2}B^2} \tag{3.2}$$

$$F_{22} = -9.80 \times 10^{-4}\ \frac{n_c^2\ \ell n\Lambda}{T_c^{1/2}B^2} \tag{3.3}$$

$$F_{31} = 8.15 \times 10^{-6}\ \frac{n_c^2\ \ell n\Lambda}{T_e^{3/2}B^2} \tag{3.4}$$

$$F_{32} = -1.63 \times 10^{-5}\ \frac{n_c^2\ \ell n\Lambda}{T_e^{3/2}B^2} \tag{3.5}$$

$$F_{33} = -1.63 \times 10^{-5}\ \frac{n_c\ \ell n\Lambda}{T_e^{3/2}B^2}\ (3T_e - T_c) \tag{3.6}$$

$$F_{42} = -6.33 \times 10^{-4} \frac{n_c n_\alpha \ell n\Lambda}{T_c^{3/2} B^2} \left(\frac{3.5A_i + 2}{A_i + 4}\right) \tag{3.7}$$

$$F_{43} = 1.26 \times 10^{-3} \frac{n_\alpha \ell n\Lambda}{T_c^{1/2} B^2} \tag{3.8}$$

$$- 1.65 \times 10^{-5} \frac{n_\alpha \ell n\Lambda}{T_e^{3/2} B^2} (3T_e - T_c)$$

$$F_{44} = -6.33 \times 10^{-4} \frac{n_c \ell n\Lambda}{T_c^{1/2} B^2} - 1.65 \times 10^{-5} \frac{n_c \ell n\Lambda}{T_e^{1/2} B^2} \tag{3.9}$$

All other elements of $\bar{\bar{F}}$ are zero. Temperature is is eV, density is in cm^{-3}, and time is in seconds.

III-B. Neoclassical Diffusion

If the ambipolar potential, $\phi_e(r)$, has a strong radial dependence, a particle can diffuse resonantly in the radial direction. Local cancellation of the azimuthal drift caused by the radial electric field and $\overline{\nabla}B$ can lead to neoclassical diffusion for large values of β_c. Formal calculations of the neoclassical and resonant transport and rough estimates of the diffusion coefficient for the central-cell ions have been made by Ryutov and Stupakov.[8,9] These are given in Table 3. The qualitative shape of the ion diffusion coefficient is shown in Fig. 2 and Fig. 3 as a function of the ion-ion collision frequency ν_i. The two experimental devices, TMX and PHAEDRUS, and the two tandem reactor designs should both confine plasmas with ions dominated by resonant plateau transport and electrons dominated by neoclassical plateau transport. The radial confinement time predicted for these devices based upon resonant transport for ions and neoclassical plateau transport for electrons, $\tau_\perp^{rp}$, is compared to the calculated axial confinement time, $\tau_{\parallel}$, and the classical radial confinement time, $\tau_\perp^{cl}$, in Table 4. We see

Table 3

Neoclassical and Resonant Diffusion Coefficients for Central Cell Ions in a Tandem Mirror

Type	β	Regime	Collisionality	D
Neoclassical	High	Banana	$\xi < \alpha^{3/2}$	$\alpha^{1/2} r^2 \nu_i$
		Plateau	$\alpha^{3/2} < \xi < 1$	$\alpha^2 r^2 / \tau_{dr}$
		Collisional	$\xi > 1$	$\alpha^2 r^2 / (\nu_i \tau_{dr}^2)$
	Low	Collisionless	$\xi < 1$	$\alpha^2 r^2 \nu_i$
		Collisional	$\xi > 1$	$\alpha^2 r^2 / (\nu_i \tau_{dr})^2$
Resonant	--	Banana	$\eta < (\frac{\delta r}{r})^{3/2}$	$r^2 (\frac{\delta r}{r})^{1/2} \nu_i$
		Plateau	$\eta > (\frac{\delta r}{r})^{3/2}$	$\frac{\delta r^2}{\tau_{\parallel}}$

$\xi = \nu_i \tau_{dr}$; $\eta = \nu_i \tau_{\parallel}$; τ_{dr} = azimuthal drifting period; $\tau_{\parallel}$ = bounce period; $\alpha = \frac{L_{tr} r}{L} (\frac{r}{L_{tr}})^4$; $\delta r \sim \frac{\rho_i r}{L_{tr}}$; ρ_i = ion gyro radius; L_{tr} = length of the transition zone; L = length of the central cell; r = radius of the central cell.

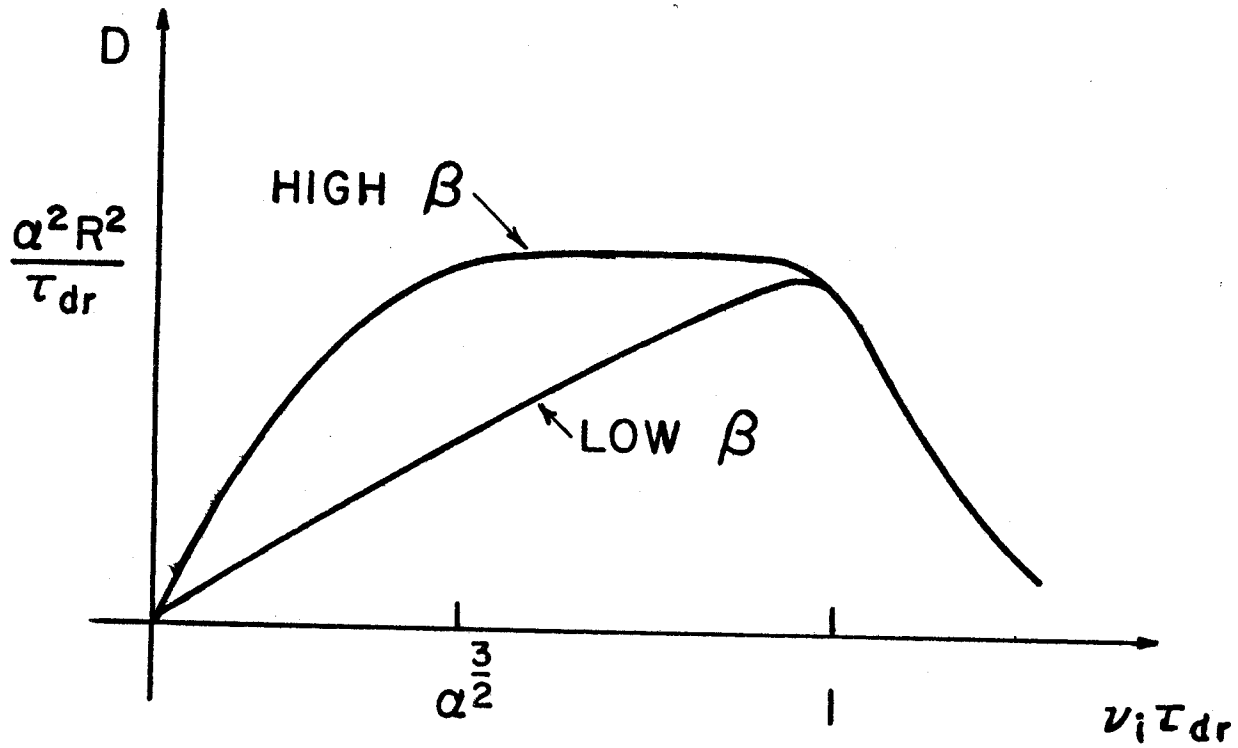

Fig. 2 Qualitative dependence of the neo-classical diffusion coefficient on the collision frequency

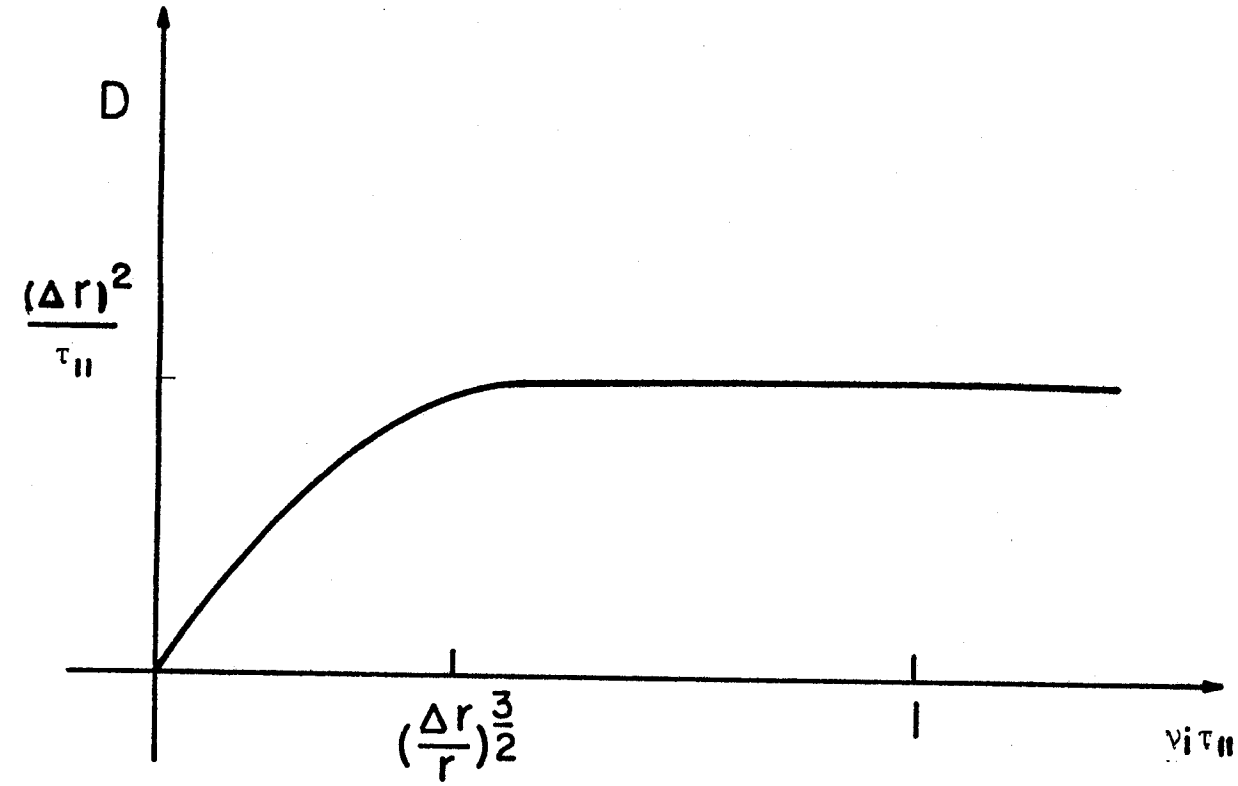

Fig. 3 Qualitative dependence of the resonant diffusion coefficient D as a function of ion collision frequency ν_i

Table 4

Comparison Between Resonant Plateau Transport and Axial Confinement for Central Cell Ions in a Tandem Mirror

cm^{-3}-sec	TMX	PHAEDRUS	TMR-LLL	TMR-UW
$(n\tau)_{\perp}^{rp}$	1×10^{12}	1×10^{11}	4×10^{15}	2×10^{15}
$(n\tau)_{\perp}^{cl}$	4×10^{12}	7×10^{11}	6×10^{17}	3×10^{17}
$(n\tau)_{\parallel}$	3×10^{11}	3×10^{10}	8×10^{14}	8×10^{14}

that the radial confinement time, $\tau_{\perp}^{rp}$ is only a factor of 3 to 5 greater than the axial confinement time. Thus, radial losses will not be negligible.

IV. Numerical Solution of the Fluid Model Equations

The basic set of transport equations (eqns (2.11, 2.12, 2.21, 2.38 and 2.39)) consists of three non-linear partial differential equations describing central cell plasma and two non-linear ordinary differential equations describing the plug plasma. The two sets of equations are coupled by the term in the electron energy balance equation which describes energy transfer between the ions in the end plugs and the electrons. The two sets of equations have two different characteristic times. The plug ions are confined magnetically. Therefore, the plug plasma density and ion energy vary more rapidly than the density and temperature of the central cell ions or the temperature of the electrons. This allows one to use well-developed tokamak transport codes to model the central cell tandem mirror plasma without major modifications of the code itself. The central cell equations are similar in form to the transport equations of a tokamak except for the following items:

1. The presence of the axial loss terms in the density and in the energy equations.

2. The terms in the electron energy equation which account for the electrons in the plugs. These are roughly smaller by the ratio of the plug volume to the central cell volume.

Furthermore, the central cell plasma is cylindrical over most of its volume which makes the use of cylindrical coordinates (the standard system in tokamak modeling programs) a quite proper choice. In this section, we consider as an example numerical solutions of these equations using the

Wisconsin tokamak transport code[18] and classical transport coefficients. The machine parameters are those characterizing the PHAEDRUS tandem mirror experiment.

IV-A. Effects of Boundary Conditions

The boundary conditions at the axis of the central cell are that the particle and energy flux must vanish, i.e.,

$$\begin{bmatrix} Q_e \\ Q_i \\ \Gamma_i \\ \Gamma_\alpha \end{bmatrix}_{r=0} = 0 \tag{4.1}$$

At the plasma edge, the boundary conditions for the particle density and temperature are of the form

$$\alpha A + \beta \frac{\partial A}{\partial r} = \gamma \tag{4.2}$$

The usual choices are either to fix the parameter or its logarithmic derivative, that is, to choose either

$$\beta = 0 : \quad A\Big|_{r_{max}} = A(r_{max}) \tag{4.3}$$

or

$$\gamma = 0 : \quad \frac{1}{A}\frac{\partial A}{\partial r}\Big|_{r_{max}} = -\frac{1}{\Delta_A} \tag{4.4}$$

Both fixed and logarithmic boundary conditions are studied here. For fixed boundary conditions, the density and temperature of the central cell plasma at the edge are set at constant, low values. For logarithmic boundary conditions, the extrapolation lengths, Δ, are set equal to 3 cm

in all cases. The equilibrium radial profiles which have been found are shown in Figs. 4a and 4b. The plug plasma density and ion energy are assumed to vary radially as given by equations (2.36) and (2.37) with m=1 and n=0.1. For PHAEDRUS, the solutions obtained are not sensitive to the type of boundary conditions chosen.

IV-B. Effects of Classical Radial Transport

The equilibrium plasma parameters obtained with transport coefficients scaled classically are listed on Table 5. In Figs. 5a and 5b, the equilibrium radial profiles of various plasma parameters for PHAEDRUS are shown for two cases in which the transport coefficients are 1 and 10 times the classical values, respectively. All cases had identical initial conditions, the same amount of injected power into the plug plasma, and the same amount of central cell plasma fueling. The plug parameters are assumed to vary radially as given by equations (2.36) and (2.37) with m=1, n=0.1. Fixed boundary conditions are used. As the transport coefficients are increased above the classical values, the profiles become flatter. The dominant radial transport is due to ion conduction. A higher ion conductivity and a higher diffusion coefficient lower the central-cell ion temperature T_c. Since the central cell axial confinement time varies as $\frac{z\, e\phi_c}{T_c} \exp\frac{z\, e\phi_c}{T_c}$, lower values of T_c lead to better central cell axial confinement. Therefore the electron temperature T_e is higher and this in turn causes the plug as well as the central cell axial confinement time to again increase. The relative fraction of energy and particle losses through various radial and axial transport processes for classical and ten times classical radial transport are given in Table 6. When the radial transport is classical,

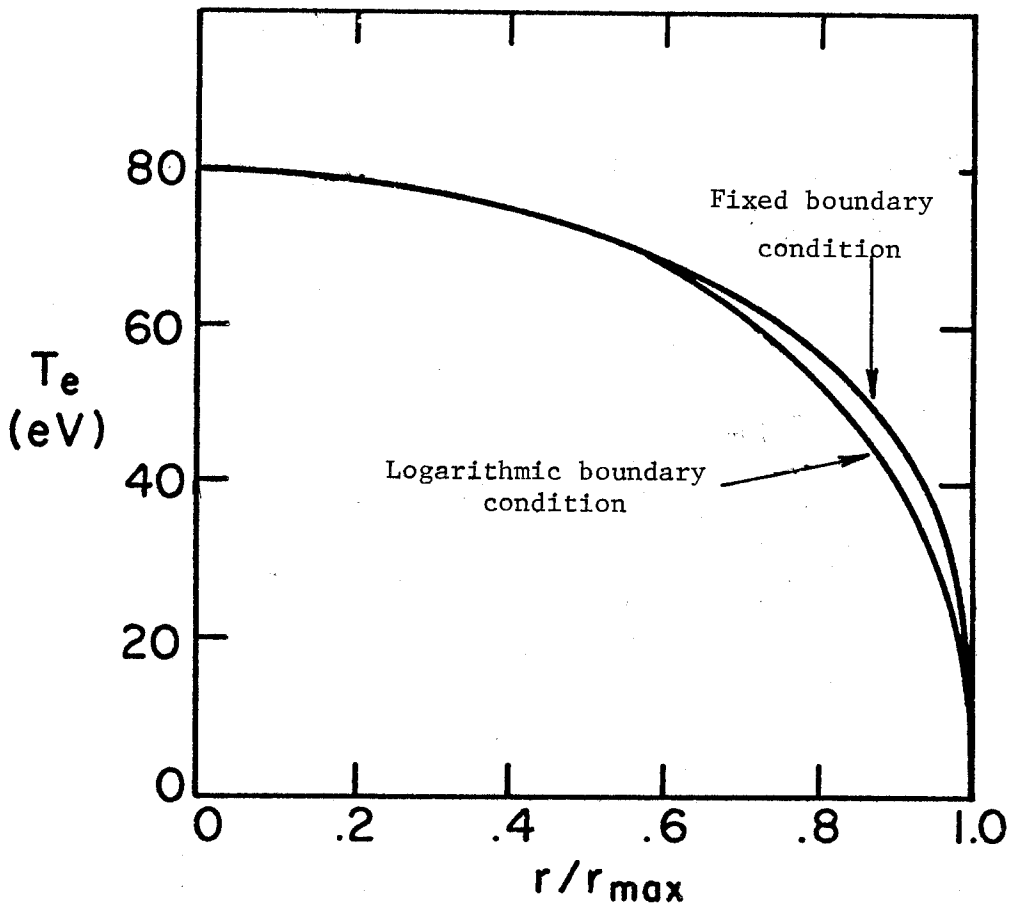

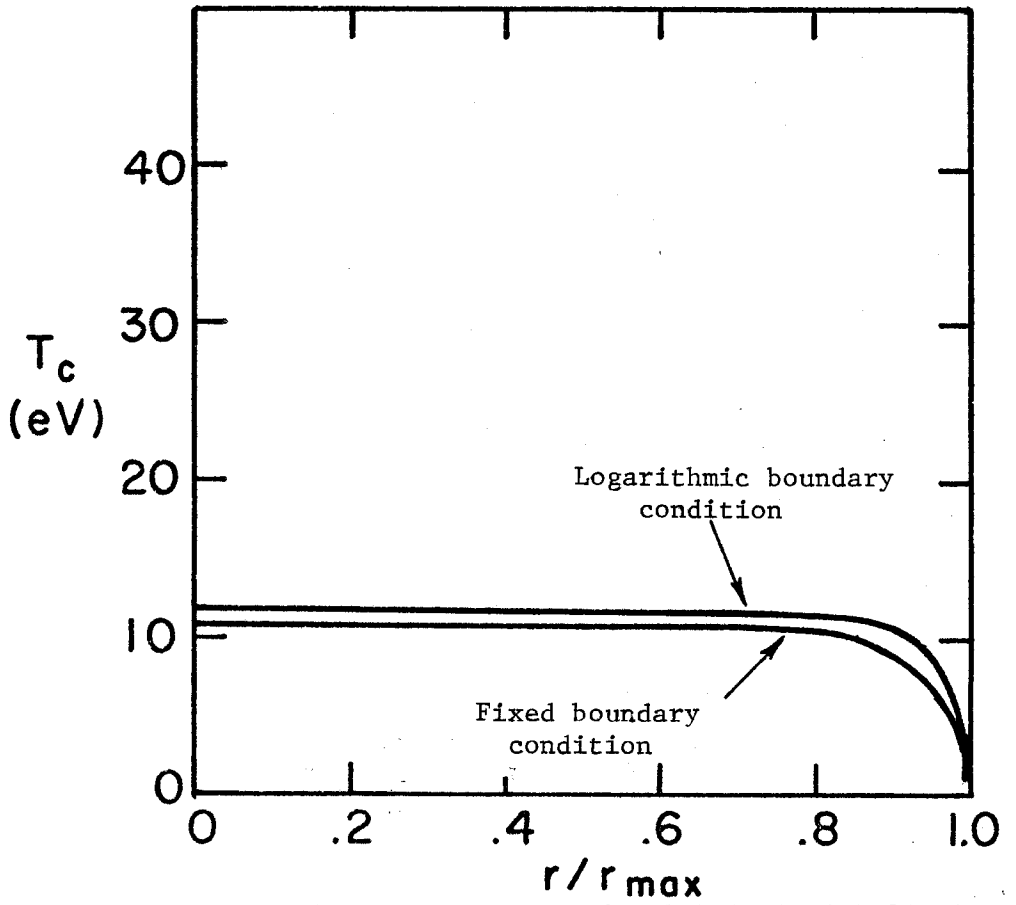

Fig. 4a Equilibrium profiles for PHAEDRUS with 10 times classical transport coefficients

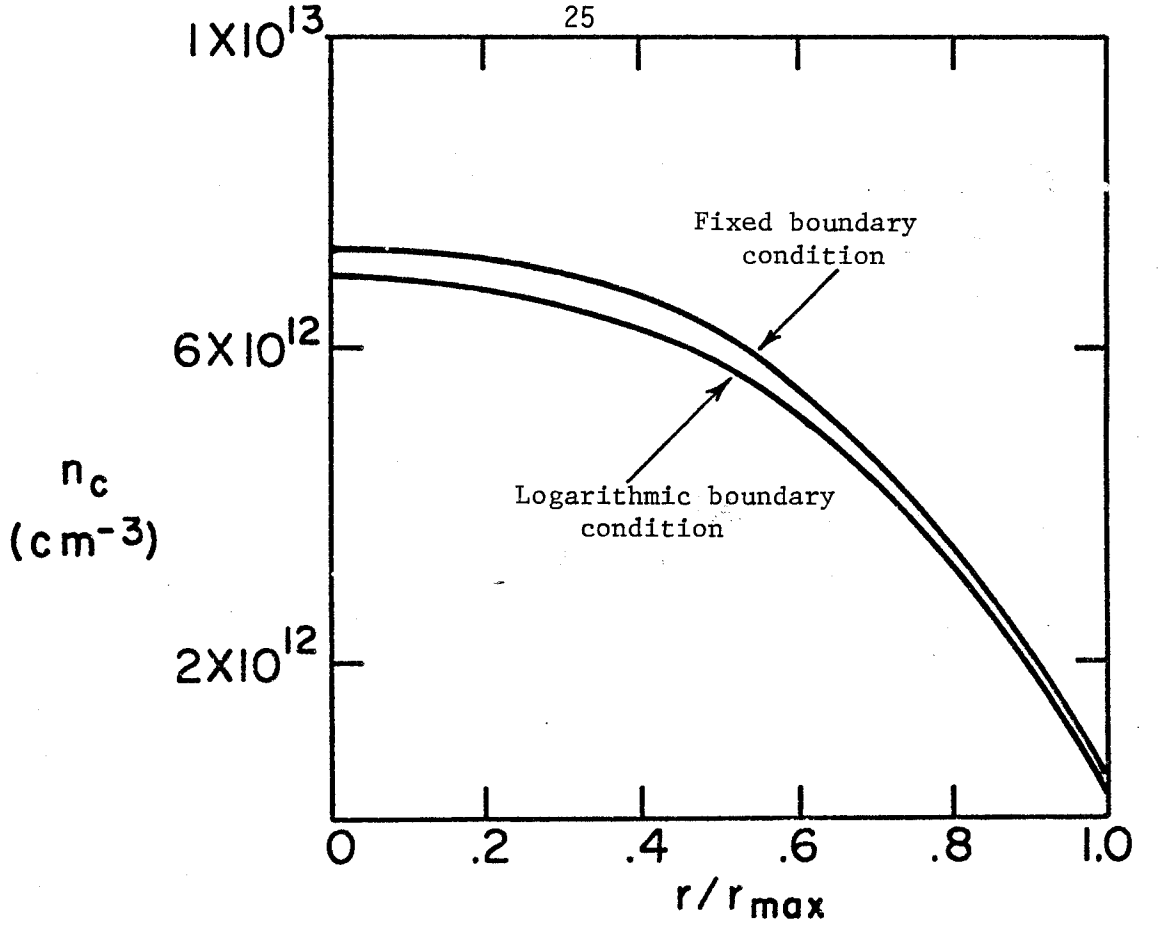

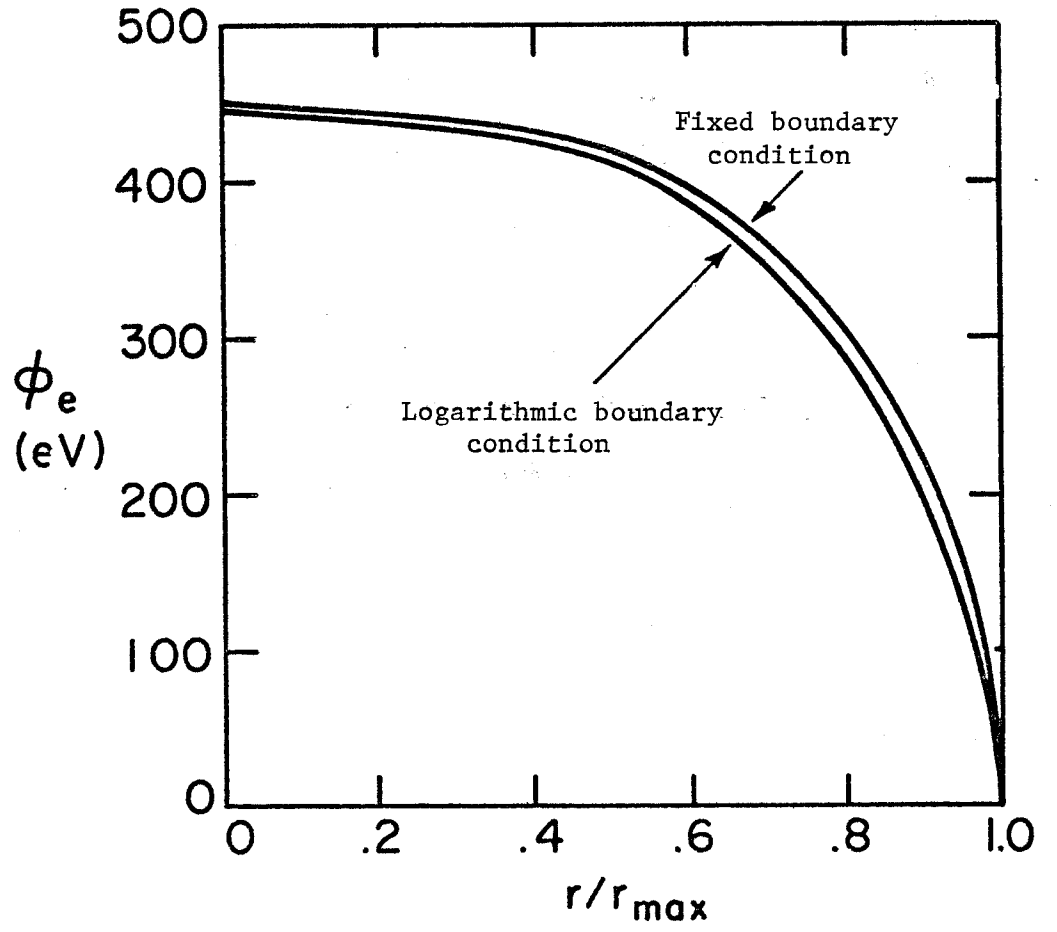

Fig. 4b Equilibrium profiles for PHAEDRUS with 10 times classical transport coefficients

Table 5

Influence of Radial Transport on Various Plasma Parameters

Levels of Transport in Central Cell

	$0.1(D_{c1}, X_{c1})$	(D_{c1}, X_{c1})	$5(D_{c1}, X_{c1})$	$10(D_{c1}, X_{c1})$
$n_p(cm^{-3})$	9.8×10^{12}	1.0×10^{13}	1.05×10^{13}	1.12×10^{13}
$E_p(keV)$	2.4	2.4	2.44	2.5
$n_c(cm^{-3})$	4.0×10^{12}	4.0×10^{12}	4.2×10^{12}	4.25×10^{12}
$T_c(eV)$	17	17	15.6	10.5
$T_e(eV)$	54	56	60	66
$\phi_e(eV)$	298	305	333	381
$\phi_c(eV)$	49	51	54.3	62.3

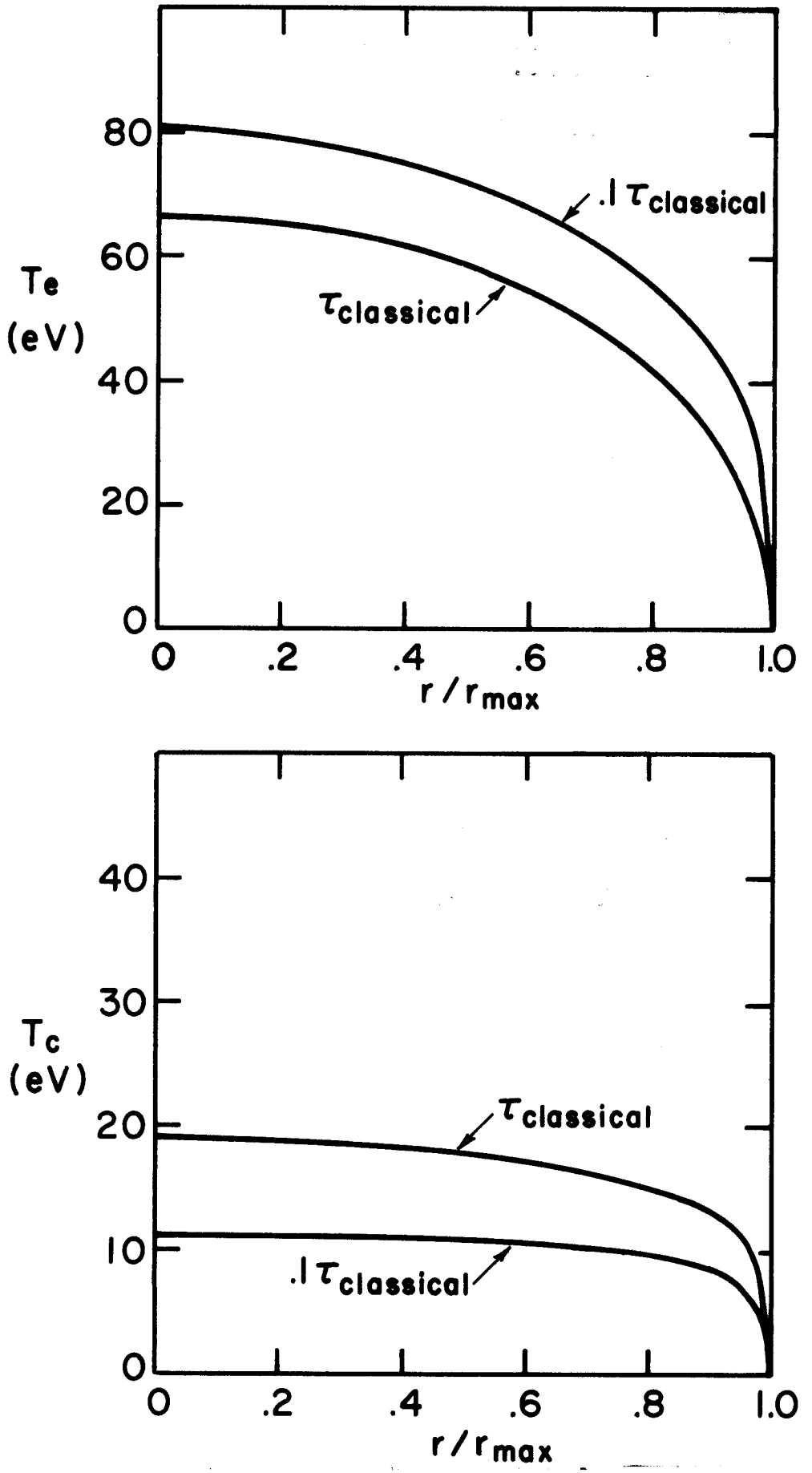

Fig. 5a Equilibrium profiles for PHAEDRUS, m = 1., n = 0.1, fixed boundary conditions

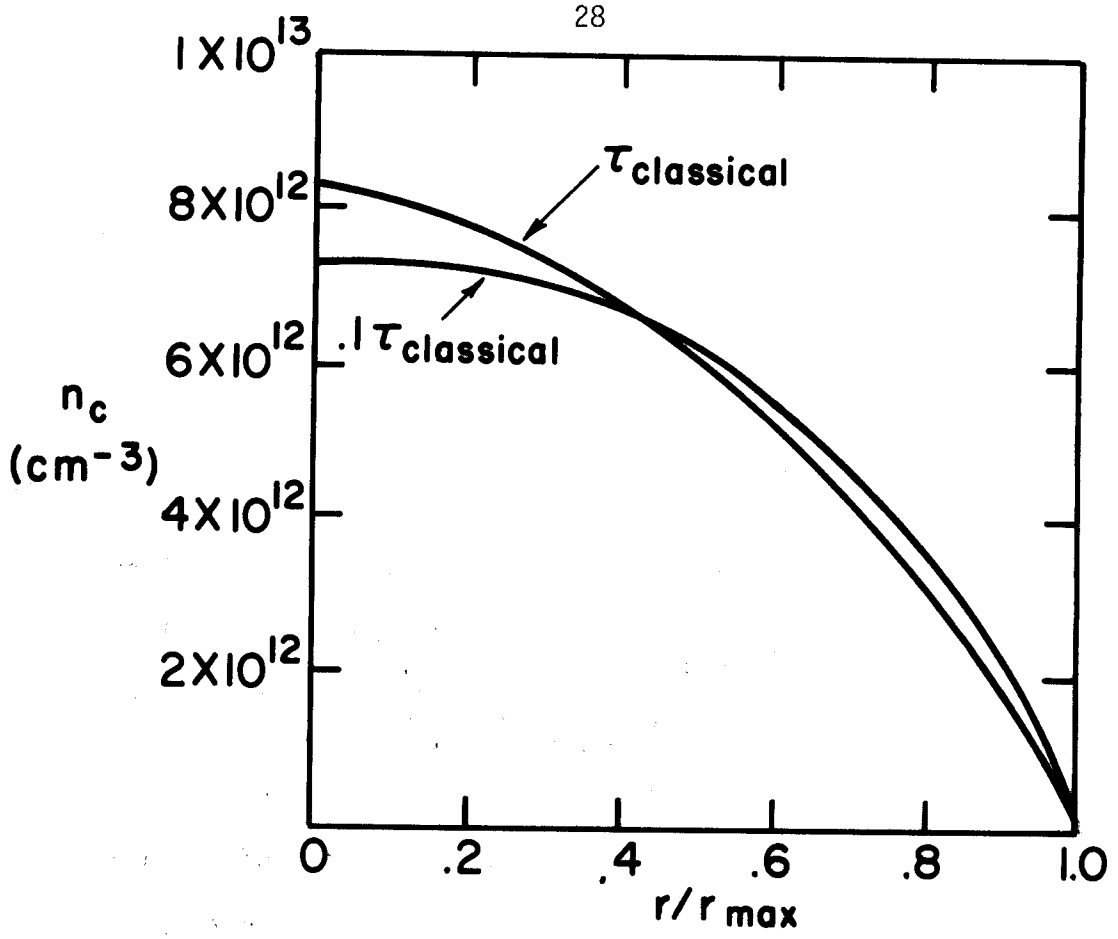

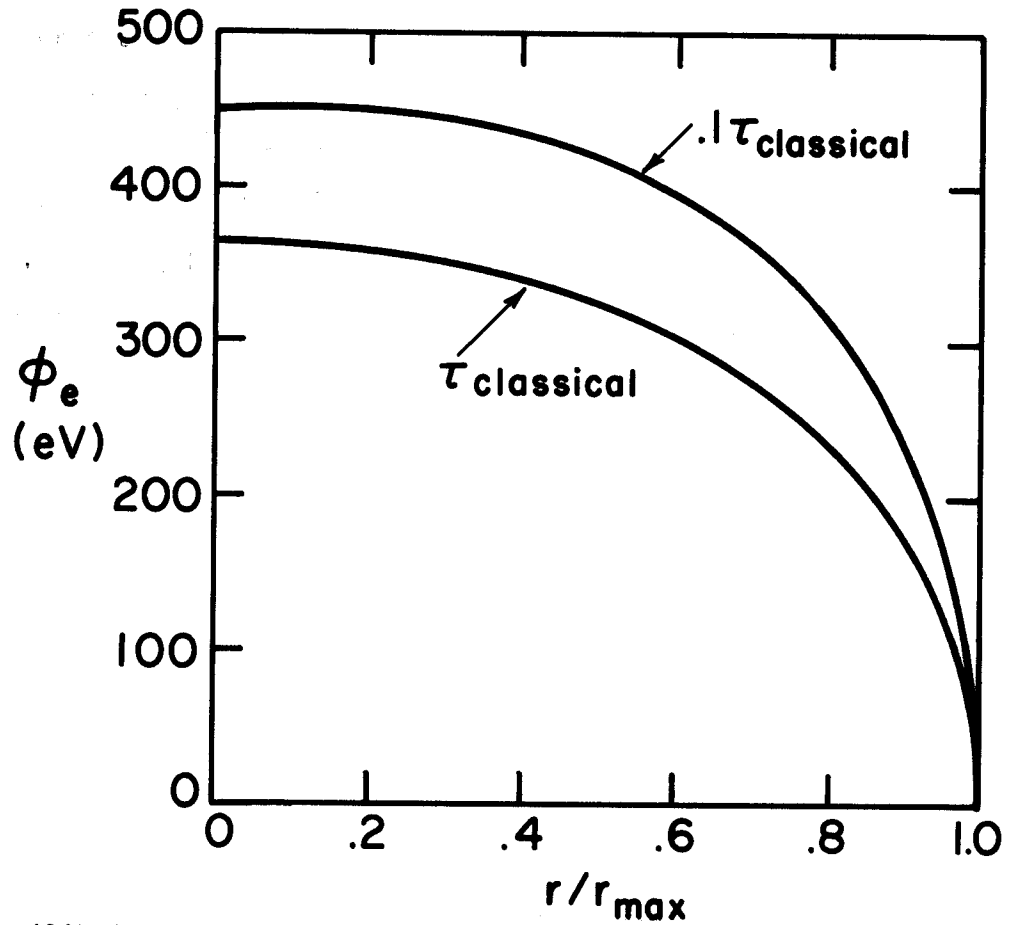

Fig. 5b Equilibrium profiles for PHAEDRUS, m = 1.,n = 0.1, fixed boundary conditions

Table 6

Relative Fraction of Particle and Energy Losses for PHAEDRUS When the Transport Coefficients are 1 and 10 Times the Classical Values

	(D_{cl}, X_{cl})	$10(D_{cl}, X_{cl})$
radial ion conduction	0.050	0.79
radial ion convection	0.005	0.02
axial loss	0.945	0.19
radial electron conduction	6×10^{-4}	0.04
radial electron convection	0.01	0.23
radiation	10^{-5}	5×10^{-5}
ion drag	0.19	0.39
axial loss	0.80	0.34
axial particle loss	0.98	0.47
radial particle loss	0.02	0.53

particle and energy losses are mainly in the axial direction. When the radial transport is ten times the classical value, radial losses become dominant.

IV-C. Effect of Plug Radial Profiles

The plug density and energy are assumed to vary radially as given by equations (2.36) and (2.37). We examine here the effects of different plug radial density profiles on the equilibrium central cell radial profiles. Typically the plug radial energy profile is relatively flat so that n in equation (2.37) is set equal to 0.1. In Figs. 6a and 6b the equilibrium radial profiles of the electron temperature, central cell ion temperature and density and the ambipolar potential of the central call with respect to ground are shown for two different radial plug density profiles: parabolic (m=1) and flat (m=0.2). The calculated equilibrium profiles of the central cell plasma tend to follow the plug density profile. In particular, for the case m=0.2, the ambipolar potential $\phi_e(r)$ is flat over most of the central cell volume. This means that the radial electric field is weak everywhere inside the plasma except near the boundary.

IV-D. Discussion

The calculations for the Wisconsin tandem mirror device, PHAEDRUS, using classical transport scaling show that the radial profiles of various central cell plasma parameters can be controlled by tailoring the plug plasma density profile. In particular, the radial electric field inside the plasma in the central cell can lead to rotation-driven instabilities.[20] The radial electric field can be eliminated by keeping the plasma density profile moderately flat(m=0.2)in equation (2.37). . If the radial

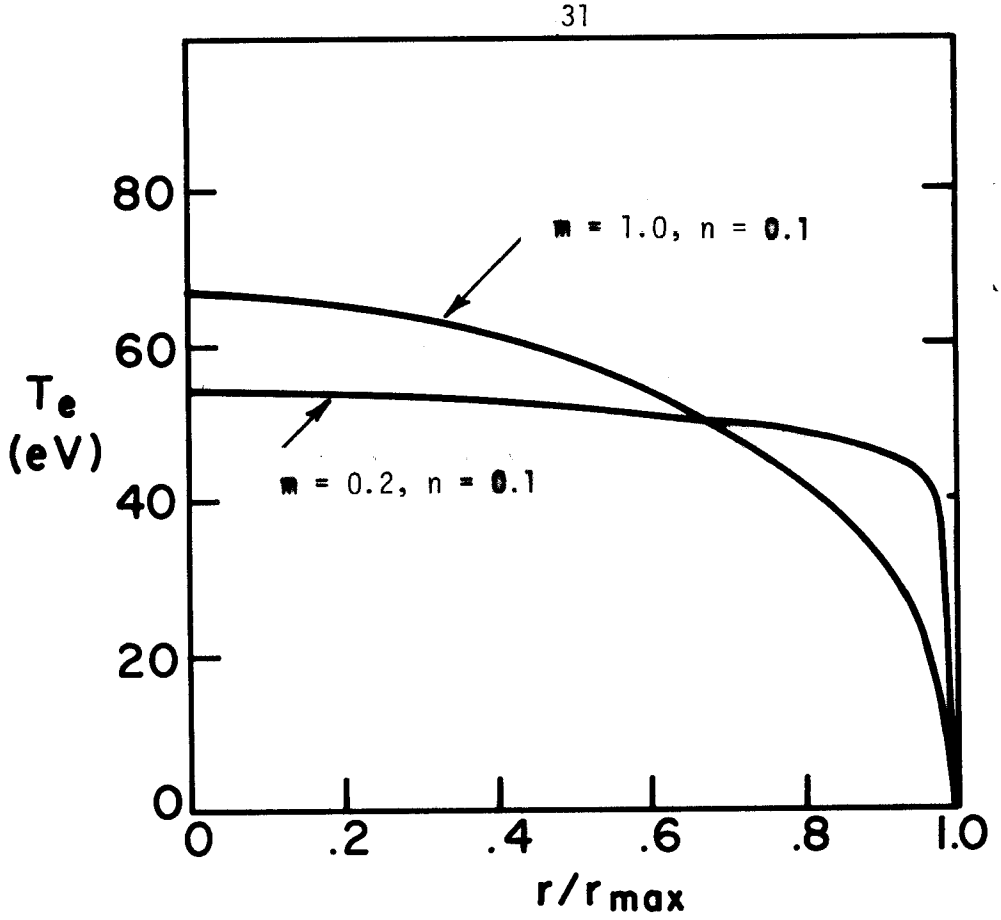

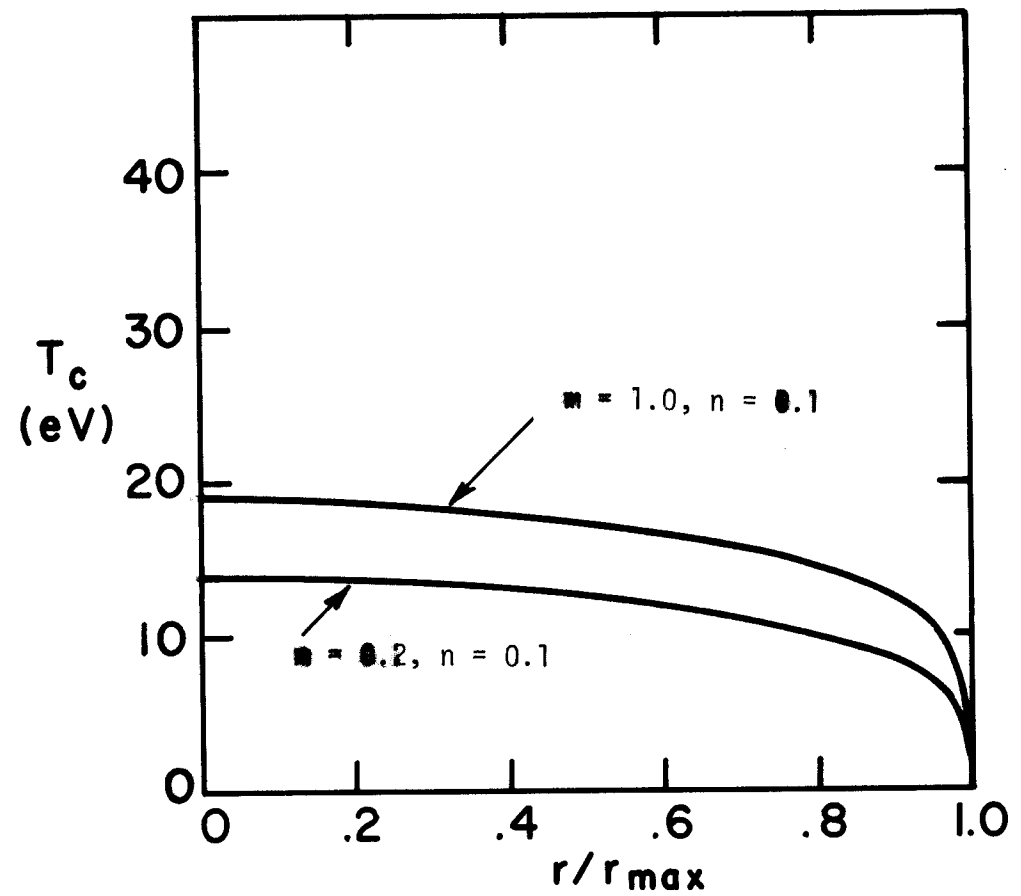

Fig. Equilibrium profiles for PHAEDRUS, classical transport, fixed boundary conditions

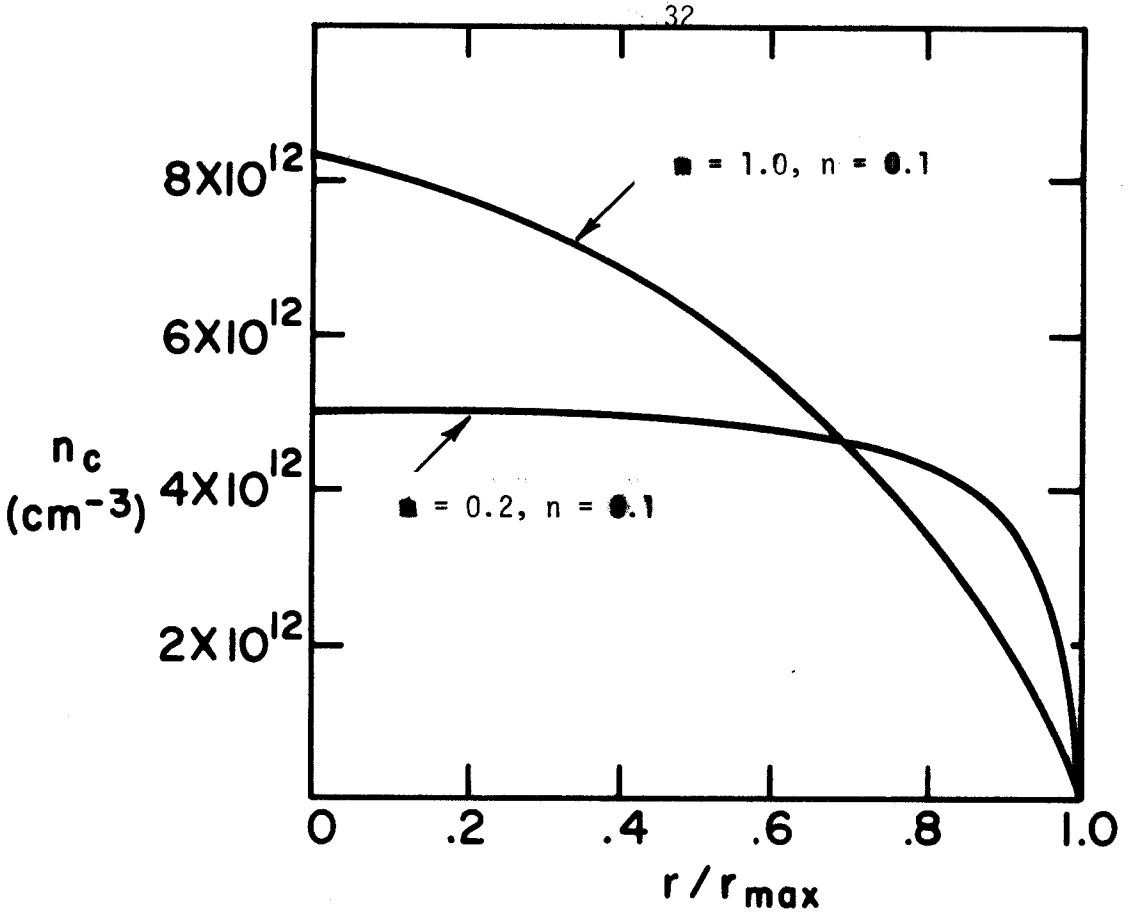

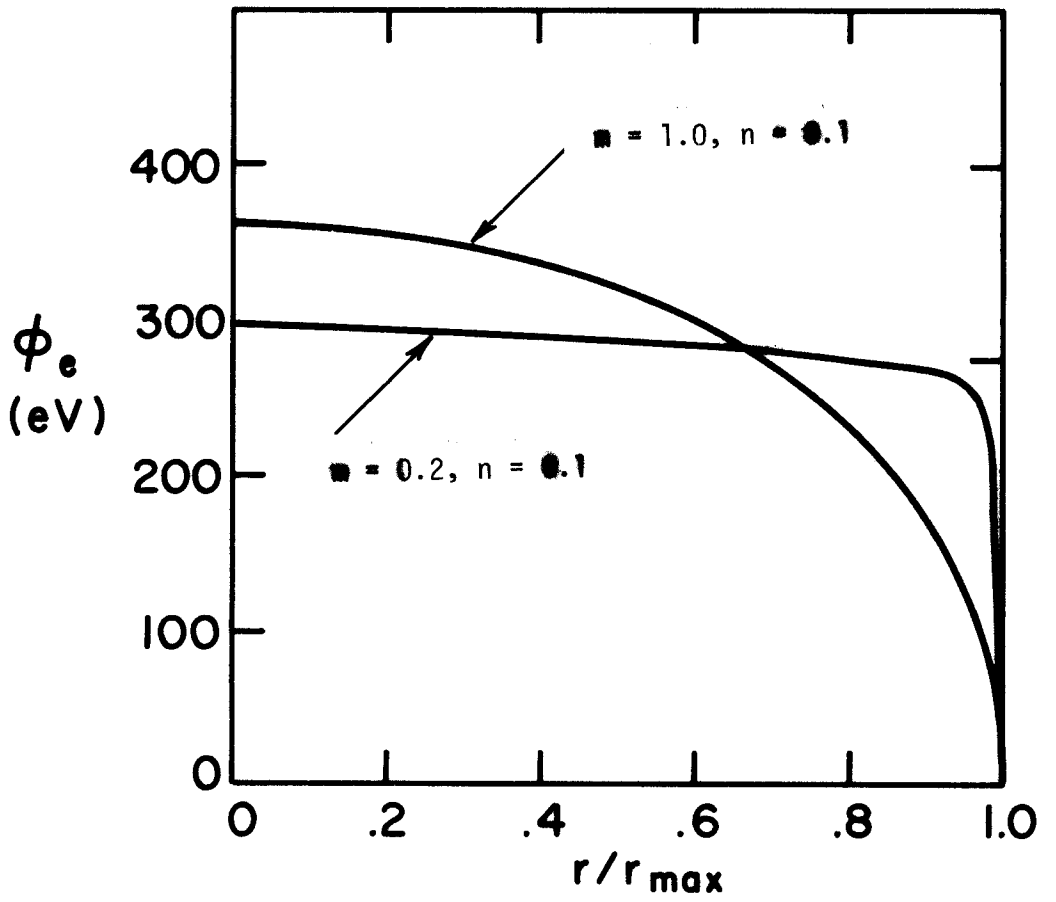

Fig. ■ Equilibrium profiles for PHAEDRUS, classical transport, fixed boundary conditions

transport in the central cell is classical, most of the particle and energy losses are in the axial direction. If the radial transport is anomalous and the transport coefficients are a few times the classical values, the losses are then mainly in the radial direction. Finally, for PHAEDRUS, the plasma conditions at the edge are not found to influence the plasma parameters in the central region.

V. Summary

We have developed a fluid model for plasma confined in the central cell of a tandem mirror. The model properly includes the axial losses, the radial losses, and the interaction of the electrons with all the ionic species in the central cell and in the plugs. The plug plasma density and ion energy are self-consistently calculated with either fixed or calculated profile shapes. The radius of each differential flux tube in the plug is related to those in the central cell by conservation of magnetic flux. The ambipolar potential of the central cell with respect to ground, ϕ_e, is determined at each radial position by equating the total electron and ion fluxes from each of these differential flux tubes. Calculations are then performed for the Wisconsin tandem device PHAEDRUS using classical radial transport coefficients. The results show that in tandem mirror experiments, the radial profiles of various central-cell plasma parameters can be controlled by tailoring the plug plasma density profile. If the radial transport coefficients are eight to ten times the classical values, the losses are mainly in the radial direction. For PHAEDRUS, the results are not sensitive to whether a fixed or logarithmic boundary condition is used.

Acknowledgement

Support for this work was provided by the U.S. Department of Energy.

References

1. G. I. Dimov, V. V. Zakaidakov, M. E. Kishinevsky, Plasma Physics and Controlled Nuclear Fusion Research (Proc. 6th Int. Conf. Berchtesgaden, 1976) 3, IAEA, Vienna (1977) 177.

2. T. K. Fowler, B. L. Logan, Comments on Plasma Physics and Controlled Fusion Research, Volume II, No. 6 167 (1977).

3. F. H. Coensgen et al., Lawrence Livermore Laboratory TMX Major Project Proposal LLL-Prop-148 (1977).

4. R. S. Post, J. Kesner, J. Scharer, R. W. Conn, Bull. Am. Phys. Soc. 22, 1094 (1977).

5. R. W. Moir et al., Lawrence Livermore Laboratory Report UCRL-52303 (1978).

6. K. C. Shaing, R. W. Conn, J. Kesner, Bull. Am. Phys. Soc. 23, 882 (1978).

7. L. L. Lao, R. W. Conn, J. Kesner, Nucl. Fusion, 18 (1978) 1308.

8. D. D. Ryutov, G. V. Stupakov, Fiz. Plazmy, 4 (1978) (in press).

9. D. D. Ryutov, G. V. Stupakov, Dokl. Akad. Nauk. 240 (1978) (in press).

10. V. P. Pastukhov, Nucl. Fusion 14 (1974) 3.

11. R. H. Cohen, M. E. Rensink, T. A. Cutler, A. A. Mirin, Nucl. Fusion 18 (1978) 1229.

12. D. P. Chernin, M. N. Rosenbluth, Nucl. Fusion 18 (1978) 47.

13. R. H. Cohen, Lawrence Livermore Laboratory Report UCRL-81795 (1978) (submitted to Nuclear Fusion).

14. S. I. Braginskii, Rev. of Plasma Phys., 1 (1965) 205.

15. M. N. Rosenbluth, A. N. Kaufman, Phys. Rev. 109 (1958) 1.

16. J. B. Taylor, Phys. Fluids, 4 (1961) 1142.

17. C. L. Longmire, M. N. Rosenbluth, Phys. Rev. 103, (1956) 507.

18. W. A. Houlberg, R. W. Conn, Nucl. Sci. Eng. 64 (1977) 141.

19. A. T. Mense, Nucl. Eng. Dept., Univ. of Wisconsin Report UWFDM-219 (1977)

20. D. E. Baldwin et al., Plasma Physics and Controlled Nuclear Fusion Research (Proc. 7th Int. Conf. Innsbruck 1978) Paper CN-37/J-4.